https://doi.org/10.5194/egusphere-2025-2722
Preprint. Discussion started: 7 July 2025


# Spatial variability in bedload transport rates determined by river pattern

Laura Quick[1,5], Trevor B. Hoey[2], Richard David Williams[1], Richard J. Boothroyd[3], Pamela M.L. Tolentino[1], Carlo P.C. David[4]

[1]School of Geographical and Earth Sciences, University of Glasgow, Glasgow, G12 8QQ, United Kingdom
[2]Department of Civil and Environmental Engineering, Brunel University of London, Uxbridge, UB8 3PH, United Kingdom
[3]Department of Geography and Planning, University of Liverpool, Liverpool, L69 7ZT, United Kingdom
[4]National Institute of Geological Sciences, University of the Philippines, Diliman, Quezon City, 1101, Philippines
[5]College of Science and Engineering, University of Edinburgh, Edinburgh, EH9 3JY, United Kingdom

*Correspondence to*: Richard D. Williams (richard.williams@glasgow.ac.uk)

**Abstract.** Local spatial patterns in flow hydraulics generate temporal variations in bedload transport rates. The nature of this local spatial variability changes as larger spatial scales are considered. Here, we investigate the hypothesis that spatial variability in bedload transport is a function of river pattern defined at the reach scale. A high-resolution system-scale DEM, which fuses bathymetric and topographic surveys, is used for two-dimensional hydraulic modelling to predict distributions of flow depth, velocity and shear stress. From this modelling, we predict bedload transport rates in four contiguous reaches with different (meandering, wandering, braided, deltaic) river patterns. Spatial and frequency distributions of bedload transport rate reveal distinct signatures associated with each river pattern. The results enable the real-world variance in the continuum of river patterns and bedload transport to be characterised, with implications for assessing channel change from, for example, anthropogenic modification and restoration.

## 1 Introduction

Fluctuations in bedload transport rates are ubiquitous in time series data and are fundamental to understanding bed material transport dynamics (Ancey, 2020). Although dependent on measurement methodology, these fluctuations scale with transport rate and influence the morphodynamics of bedforms at all scales (Ancey, 2020; Ghilardi et al., 2014; Redolfi et al., 2018). Transport rate fluctuations are frequently related to spatial patterns of transport across a riverbed at a given time (Hoey et al., 2000; Lisle et al., 2000), and the spatial variability in the hydraulics that control bedload movement is itself suggested to be a function of channel morphology (Paola, 1996; Nicholas, 2000).

Whether for defining sampling protocols (Ancey and Pascal, 2020), predicting transport rates (Adams and Eaton, 2022), determining reach-scale morphodynamic adjustments (Dhont and Ancey, 2018; Redolfi et al., 2018), assessing the

https://doi.org/10.5194/egusphere-2025-2722
Preprint. Discussion started: 7 July 2025


consequences of sediment inputs (Reiterer et al., 2025), or understanding the impacts of engineering (Lisle et al., 1997), understanding bedload transport is critical. Although monitoring instantaneous bedload transport rates across entire river reaches remains impossible, advances in fluvial remote sensing (Piegay et al., 2020) have enabled the generation of high-resolution catchment-scale Digital Elevation Models (DEMs) that incorporate river bathymetry (e.g. Lague and Feldmann, 2020). Together with estimates of surface roughness and hydrology, these DEMs can provide boundary conditions for 2D hydraulic simulation (Bates, 2022) and bedload transport prediction. Reliable, verified hydraulic models enable flow properties (i.e. water depth, velocity, shear stress) to be predicted at catchment- or reach-scale (Lisle et al., 2000; Williams et al., 2011, Segura and Pitlick, 2015), from which bedload transport rates can computed (Reid et al., 2019).

Relating channel morphology to transport dynamics first requires identification of distinct morphologies. Channel patterns lie on continua (e.g. Huang and Nanson, 2007; Brierley and Fryirs, 2005) and are increasingly being described in terms of dynamics (Boothroyd et al., 2025; Graf, 2000) rather than using temporal snapshots. Accepting that the boundaries between channel patterns may be fuzzy, contrasting channel patterns are often identifiable using different classifications and descriptive measures (e.g. Tejedor et al., 2022). This approach enables individual river reaches to be identified that have distinct morphologies and process environments (Kasprak, 2016).

We hypothesise that reach-scale spatial variability in bedload transport, expressed through probability density functions, is a function of river pattern. To test this, we numerically simulate two-dimensional flow dynamics of a gravel-bed riverscape (Fig. 1a) using a 0.5 m resolution topo-bathymetric DEM (Fig. 1c). Modelled shear stresses (Fig. 1g) are then combined with grain size observations to compute predicted bedload transport rates (Fig. 1h). We use a simplified qualitative classification of river planform morphology to define four contiguous reaches with contrasting channel patterns (Fig. 1a and 1b). Selecting multiple different reaches within a single river enables direct comparisons to be made between the four planforms, avoiding complications arising from differences in model boundary conditions between different rivers and their associated patterns. Since bedload transport remains difficult to predict (Recking et al., 2012; Recking, 2013), especially with mixed grain-sizes and complex flow histories, simplifying assumptions are required. We assume constant flow for three different magnitude flood events, grain-size distributions that are identical throughout the riverscape and which are represented by single grain sizes (i.e. D16, D50, D84), and fixed bed conditions. Together, this enables us to compare frequency distributions of these predicted bedload transport rates with each river pattern to reveal their distinct signatures.

## 2 Results

### 2.1 Area and rate of bedload transport

For all three flow magnitudes, the proportion of the riverbed where there is bedload transport (ABTA) decreases downstream from meandering (73% at $Q_{50}$) to wandering (46%), braided (20%) and deltaic (9%) patterns (Fig. 2). Only within the

https://doi.org/10.5194/egusphere-2025-2722
Preprint. Discussion started: 7 July 2025


meandering reach does the ABTA value increase significantly with discharge, rising from 66% at $Q_{10}$ to 74% at $Q_{100}$. Within all of the other pattern types ABTA remains within ±1.5% as discharge increases. Bedload transport is concentrated in one dominant channel in all reaches (Fig. 2). Bedload transport rates (Fig. 3a) also show consistent decreases from meandering (median $g_b$ = 1204 g.s$^{-1}$ at $Q_{50}$) to wandering (301 g.s$^{-1}$), braided (100 g.s$^{-1}$) and deltaic (62 g.s$^{-1}$) reaches. Median bedload transport rates and the range of these rates increase for all reaches as flow is increased (Fig. 3a).

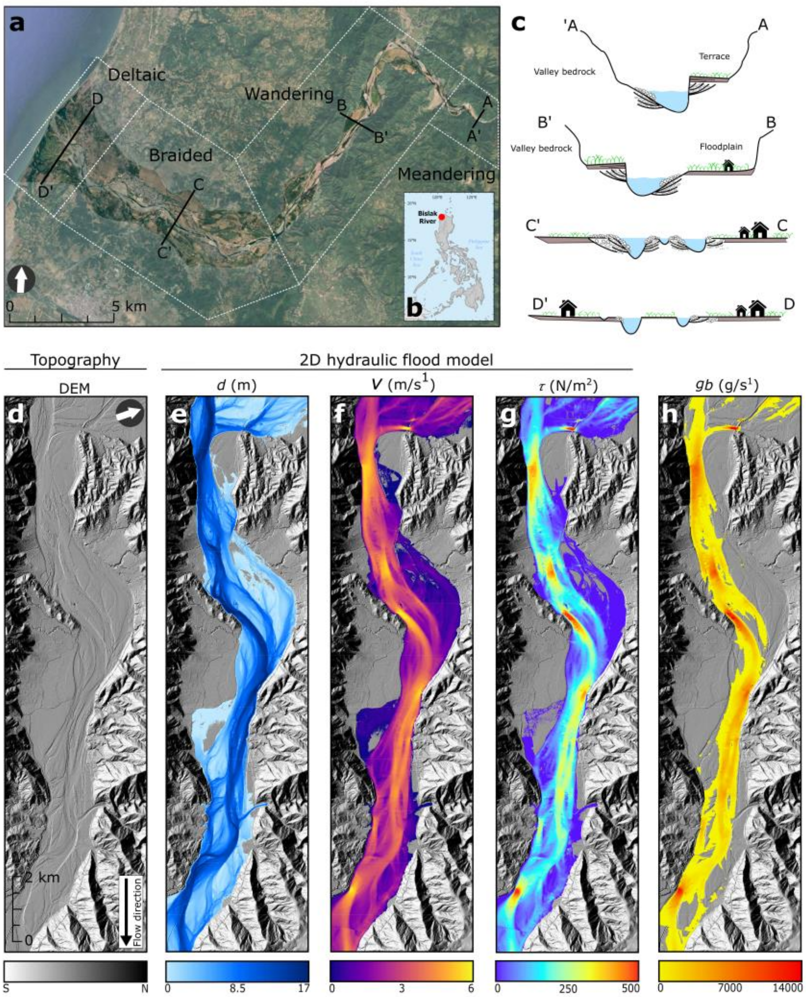


**Figure 1: a. Extent of different river patterns along the gravel-bed Bislak River, the Philippines (b). c. Conceptual cross-sections of each river pattern based on Tolentino et al. (2022). d. A section of the 2019 0.5 m resolution Bislak River DEM used for HEC-RAS hydraulic flood modelling to predict depth (e), velocity (f) and shear stress (g) for the $Q_{100}$ event. g. Bedload transport rate predictions, calculated using estimated shear stress, grain size measurements and the generalised Meyer-Peter Müller relation (Equation 1). Aerial imagery shown in (a) is © ESRI Living Atlas.**

https://doi.org/10.5194/egusphere-2025-2722
Preprint. Discussion started: 7 July 2025


The mobility of different grain sizes, uncorrected for hiding, repeats the sequence of decreasing mobility from meandering (ABTA = 73% for $D_{50}$ at $Q_{50}$) to wandering (46%), braided (20%) and deltaic (9%). There are significant changes in the mobile area for different grain sizes at the same discharge (Fig. 4). At $Q_{50}$, ABTA increases from 1% for $D_{84}$ to 28% for $D_{16}$ in the deltaic reach, and from 4% for $D_{84}$ to 45% for $D_{16}$ in the braided reach. In the meandering reach, bedload transport at $Q_{50}$ is present over higher proportions of the bed than in the multi-channel reaches, with ABTA rising from 54% for $D_{84}$ to 86% for $D_{16}$. Note that transport is longitudinally continuous for $D_{16}$ in all four patterns, regardless of flow magnitude, with discontinuities observed for both $D_{50}$ and $D_{84}$ reflecting locations where bed shear stress is below the threshold for that grain size due to low, or locally negative, bed slope. Calculated transport rates decrease with grain size (Fig. 3b), once again consistently between the four patterns.

### 2.2 Covariance of water discharge and bedload transport rates

Unit discharges of both water and bedload show visually consistent spatial patterns across all four reaches (Figs. 1d-h,2,4). These distributions are visualized using re-scaled double-mass plots (Fig. 5a-c) of cumulative bedload transport across all cells as a function of cumulative water discharge. For all flow magnitudes, relationships between cumulative bedload transport and cumulative water discharge are close to linear relationships for the meandering reach, becoming progressively more concave in the same sequence as ABTA values and bedload transport rates decrease, namely from meandering, to wandering, braided and deltaic. The greatest change in these curves (Fig. 5a-c) occurs between wandering and braided reaches.

These results illustrate the role of the excess shear stress, which depends on both discharge and grain size, in controlling bedload transport as a greater proportion of wetted cells in the braided and deltaic reaches are either below or not far above the critical stress for bedload transport. The same effect is shown by the curves for different grain-sizes (Fig. 5d-f), which represent decreasing excess stress as grain size increases. Here, close to linear curves are observed for D16 in all reaches, with the reduction in excess stress in many wetted cells for D84 shown by the concave curves for braided and deltaic reaches (Fig. 5f).

https://doi.org/10.5194/egusphere-2025-2722
Preprint. Discussion started: 7 July 2025


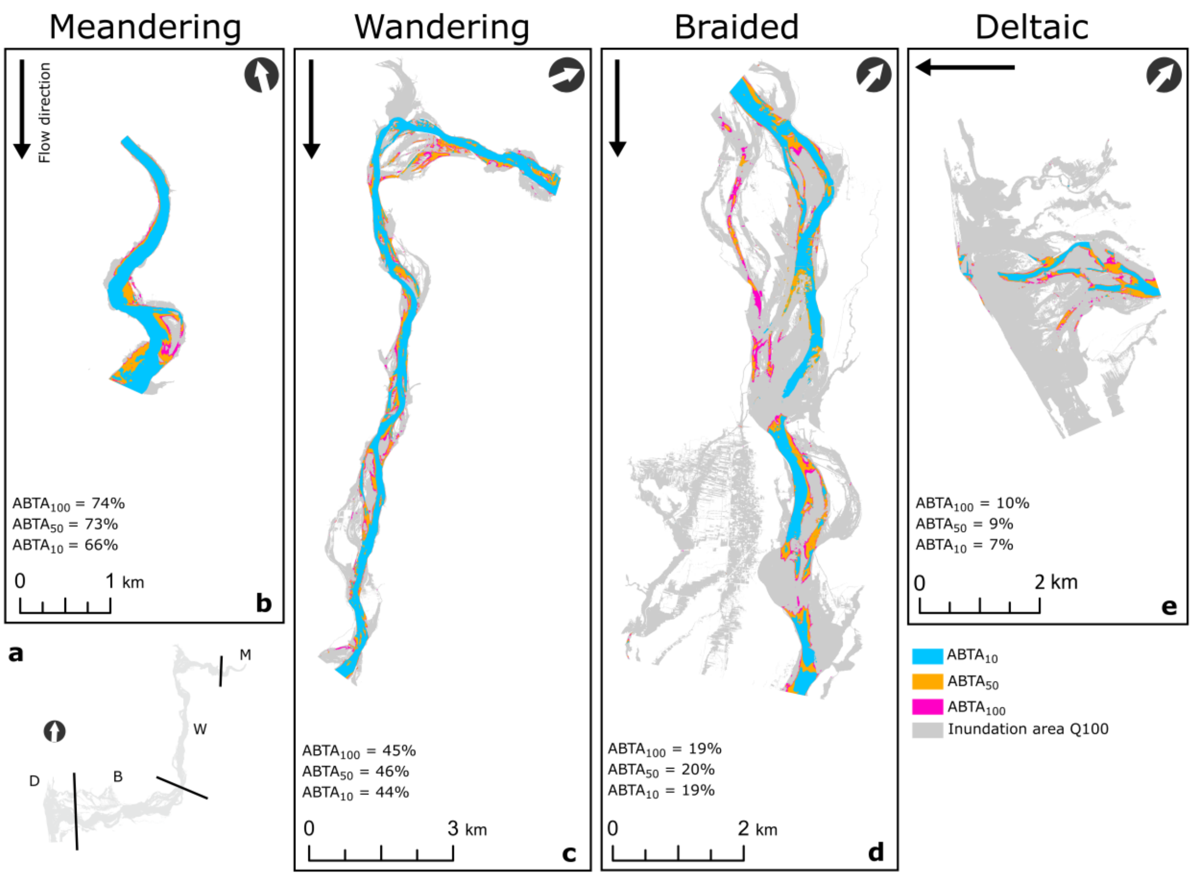


105 **Figure 2: a. Location of four different river patterns along the Bislak River (M: Meandering, W: Wandering, B: Braided, D: Deltaic). b-e. Active bedload transport area (ABTA) for each river pattern, for three flow magnitudes ($Q_{10}$, $Q_{50}$, $Q_{100}$). Grey shading shows the area of inundation for $Q_{100}$.**

https://doi.org/10.5194/egusphere-2025-2722
Preprint. Discussion started: 7 July 2025


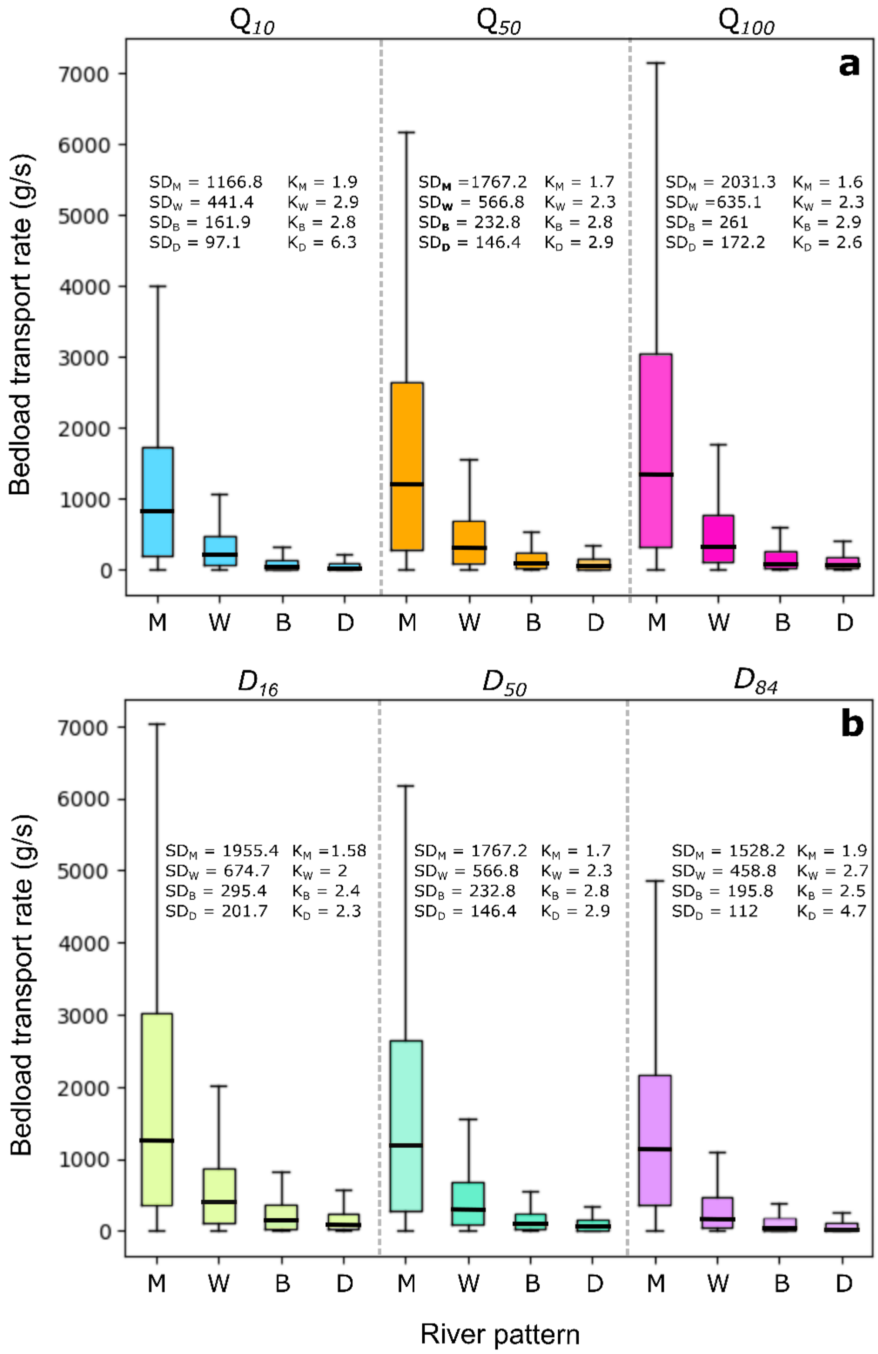


**Figure 3: Bedload transport rates for the four identified river patterns (meandering, wandering, braided, deltaic) along the Bislak River. a. Bedload transport rates for each river pattern (D50 grain size) for different flow magnitudes ($Q_{10}$, $Q_{50}$, $Q_{100}$). b. Bedload transport rates for each river pattern for a single flow magnitude ($Q_{50}$), with different grain sizes ($D_{16}$, $D_{50}$ and $D_{84}$).**

https://doi.org/10.5194/egusphere-2025-2722
Preprint. Discussion started: 7 July 2025


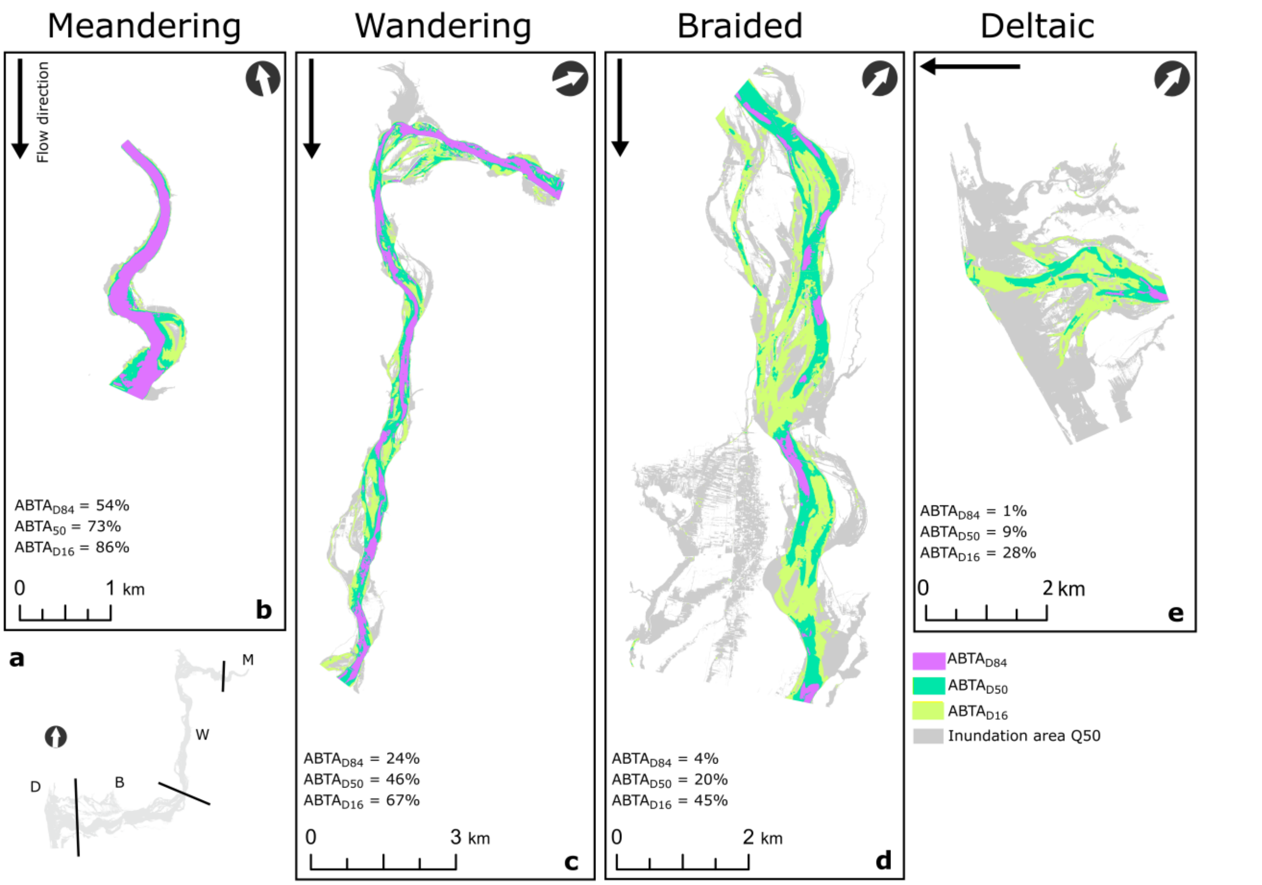


**Figure 4: a. Location of four different river patterns along the Bislak River (M: Meandering, W: Wandering, B: Braided, D: Deltaic). b-e. Active bedload transport area (ABTA) for each river pattern for a single flow magnitude ($Q_{50}$), with different uniform grain sizes ($D_{16}$, $D_{50}$ and $D_{84}$).**

## 3 Discussion

### 3.1 Spatial patterns of bedload transport

Although the total inundated area increases with flow magnitude (Fig. 2), the proportion of that inundated riverbed that experiences bedload transport (ABTA; Fig. 2) remains notably constant within each pattern type, usually concentrated within one main channel. ABTA values decrease systematically downstream as river morphology becomes less confined and the expanding flow produces shallow inundation of large areas of riverbed and floodplains that generates shear stresses below threshold. Although we have not considered transport of sediment mixtures, changing the grain size shows how the relative extent of bedload transport reduces as grain size increases (Fig. 4) through increasing the critical shear stress.

https://doi.org/10.5194/egusphere-2025-2722
Preprint. Discussion started: 7 July 2025


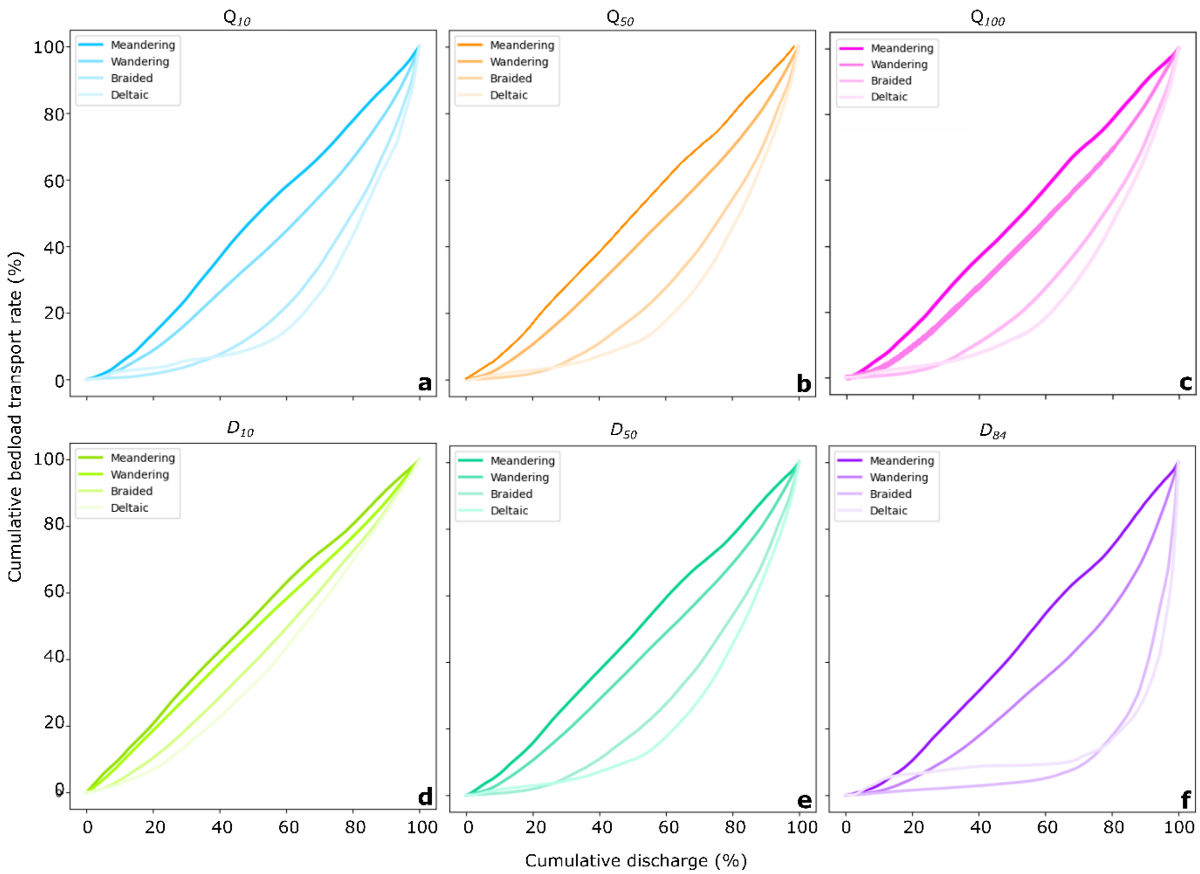


**Figure 5: Cumulative bedload transport rate against cumulative water discharge for each model cell in rank order of water discharge. All data re-scaled onto a 0-100% scale to enable comparison of the shapes of distributions. Data are shown for different discharges ($Q_{10}$, $Q_{50}$ and $Q_{100}$) (a-c) and grain sizes ($D_{16}$, $D_{50}$ and $D_{84}$) (d-f).**

Bedload transport rates calculated for single grain sizes within each reach are positively skewed, with higher median values in the meandering and wandering reaches (Fig. 3) than in the braided and deltaic reaches. In the absence of data on spatial variability of sediment size, the distributions of bedload transport rates within each reach are more informative than their absolute values. These distributions correlate with the distributions of water discharge (Fig. 5) and hence shear stress across each reach.

https://doi.org/10.5194/egusphere-2025-2722
Preprint. Discussion started: 7 July 2025


Both the locations and rates of bedload transport show significant differences between the four reaches. Whether in terms of flow magnitude or bed grain size, both inundated areas (Figs. 2,4) and transport rates (Fig. 3) show consistent changes from meandering through to deltaic patterns. These results support the initial hypothesis, and the double-mass plots (Fig. 5) demonstrate how the roles of overall mean shear stress, represented by water discharge, and critical shear stress, represented by grain size, interact to produce distinct patterns of bedload transport in the different reaches. The temporal fluctuations in transport rates that are increasingly seen as intrinsic features of bedload processes (Ancey, 2020; Paola, 1996) are thus determined by channel pattern at larger scales, consistent with formalization of bedform Church & Jones (1982) and bedload (Hoey, 1992) scales. Our results begin to quantify the influence of channel pattern on sediment transport, enabling improved understanding of the causes of unsteady sediment transport (Dhont & Ancey, 2018).

### 3.2 Controls over channel pattern

The spatial distributions of bedload transport are correlated with channel pattern and hence influence the maintenance of the morphologies of each reach. Downstream changes in channel pattern in the Bislak are related to confinement reducing downstream, resulting from both natural and anthropogenic reasons that are beyond our scope; rather, we consider the reaches as independent exemplars of different channel patterns. Progressing downstream, bedload transport occurs over a decreasing proportion of bed area, and that transport is at decreasing rates (Fig. 3). The scales of temporal variations in bedload transport will also change systematically in response to changes in flow depths and velocities, bed grain-size and consequently bedform types and sizes. As bedload transport is more size selective at lower excess stresses (Wilcock et al., 2009), local sorting of bedload and down-bar fining will become more apparent downstream (Rice & Church, 2009). Consequently, spatial patterns of deposition and erosion will determine the scale and sedimentology of sedimentary deposits formed in the different reaches (Kostic & Aigner, 2007; Rice & Church, 2009).

The concentration of bedload into dominant channels (Fig. 2) echoes analysis from braided (Ettema & Armstrong, 2019; Williams et al., 2015) and alternate bar rivers (Adams & Eaton, 2022), supporting arguments for considering channel pattern in terms of distributions of channels (Ghosh et al., 2023; Tejedor et al., 2022) or bed elevations (Andréault et al., 2024). Calibration of point-scale bedload transport relations remains challenging (Ancey, 2020; Ancey & Pascal, 2020) and improved descriptions of channel form that allow total bedload transport rates to be computed using simplified hydraulics (Adams & Eaton, 2022) would have practical benefits. Distributions of shear stress and sediment transport also inform understanding of in-stream habitats (Schwendel et al., 2010) with implications for river management and restoration.

The analysis above uses a single DEM, ignores grain sorting and makes other simplifying assumptions. There are numerous opportunities to extend this analysis, for example relating differences between successive DEMs to spatial patterns of shear stress. Ongoing improvements to data availability, including bathymetric LiDAR to accelerate DEM production (Kastdalen et al., 2024) and remotely sensed grain size (Marchetti et al., 2022), will enable refinement of the approach.

https://doi.org/10.5194/egusphere-2025-2722
Preprint. Discussion started: 7 July 2025


## 4 Conclusions

A 2D hydraulic model over a high-resolution DEM along 33 km of four distinct, contiguous reaches of a gravel-bed river was used to predict spatial patterns and frequency distributions of bed shear stress and bedload transport. Bedload is concentrated within deeper and faster flowing areas of the bed in all reaches, with excess shear stress decreasing downstream from meandering to wandering to braided and deltaic reaches. Estimated bedload transport rates also decline downstream, and double-mass plots show how bedload becomes increasingly concentrated in areas of high excess stress in the braided and deltaic reaches. Spatial variability in bedload transport is thus shown to be a function of channel pattern, with implications for our understanding of temporal variability in bedload, process-form relationships in different river patterns, design and maintenance of critical river infrastructure, and the management and restoration of riverscape habitat.

## Appendix 1: Methods

### A1.1 Study area

The gravel-bed Bislak River, the Philippines, features a longitudinal sequence of meandering, wandering, braided and deltaic channel patterns within a 33 km reach (Fig. 1A; Table S1; Tolentino et al., 2022). The confined single thread meandering reach has a moderate sinuosity main channel. The partially-confined and low sinuosity wandering reach shows a transition from single- to multi-thread channels. The braided reach contains multiple channels at all flow stages, and the deltaic reach contains multiple distributary channels. Both the braided and deltaic reaches have low overall sinuosity and are laterally unconfined. The longitudinal gradient progressively decreases downstream.

### A1.2 Topographic survey

A seamless representation of the wet and dry parts of the study area was generated by fusing an airborne LiDAR survey, echo-sounding of pools > 2 m deep and spectrally-based depth retrieval estimates (Legleiter, 2021) from orthoimagery acquired at the time of the LiDAR survey. Vertical errors are detailed in Quick et al. (2025); the dry LiDAR, echo-sounding and depth retrieval components had Root Mean Square Errors (RMSE) of 0.045, 0.250 and 0.345 m, respectively. The 12.96 $km^2$ system-scale DEM was used for two-dimensional hydraulic modelling.

### A1.3 Hydraulic modelling

Flow was simulated using the full St Venant shallow water equations in widely-used (e.g. Gori et al., 2020; Masafu et al., 2024) HEC-RAS2D. 3 m and 5 m 2D grid cells were used for the active channel and floodplain, respectively. The model was calibrated by varying Mannings n and comparing outputs to a cloud-free K3 satellite image of a 3 km long braided section acquired during the 1043 m3.s-1 Typhoon Ineng high-flow event (23/08/2019). A constant n value of 0.05 achieved a fit congruency (Bates and De Roo, 2000) of 75% (Tolentino et al., 2024), similar to that achieved for other braided rivers (e.g.

https://doi.org/10.5194/egusphere-2025-2722
Preprint. Discussion started: 7 July 2025


Williams et al., 2013). A steady-state input boundary condition used 10-, 50- and 100-year return period flows, from calibrated rainfall-runoff modelling (Paringit et al., 2017). The downstream boundary condition was normal depth. Shear stress calculations for all model cells were exported for bedload transport rate calculations.

### A1.4 Bedload transport rate

Unit bedload transport rate by mass, $g_b$, was calculated using a generalised form of the Meyer-Peter and Müller relation:

$$g_b = c[\tau - \tau_c]^k = c[g\rho RS - \tau_c]^k \quad (1)$$

where $\tau$ is bed shear stress (N.m$^{-2}$), $\tau_c$ critical shear stress (N.m$^{-2}$), $g$ acceleration due to gravity (m.s$^{-2}$), $\rho$ density of water (kg.m$^{-3}$), and $R$ hydraulic radius (m). $R$ is $A/P$, where $A$ is wetted area (m$^2$) and $P$ is wetted perimeter (m) of a grid cell face. $S$ is the slope of the energy grade line (m/m), calculated between the centres of adjacent downstream cells. The constant $c$ is set to 1 for convenience and $k$ was taken as 1.5 (results for $k$=1.8 are in SI) (Huang, 2010).

Critical shear stress, $\tau_c$, was calculated as:

$$\tau_c = \theta_c g D(\rho_s - \rho) \quad (2)$$

where $\theta_c$ is the dimensionless critical shear stress, $D$ a representative grain size (m), and $\rho_s$ particle density (kg.m$^{-3}$). Soulsby & Whitehouse's (1997) approximation of the Shields (1936) curve (equation 3) was used to calculate $\theta_c$ where $D_*$ is the dimensionless grain-size (equation 4):

$$\theta_c = [\ 0.30\ 1{+}1.2D_*] + 0.055[1- \exp(-0.020D_*)] \quad (3)$$

$$D_* = [g(s_s - 1)/v^2]^{1/3} D \quad (4)$$

where $s_s$ is $\rho_s/\rho$ and $v$ kinematic viscosity at a specific water temperature (m$^2$.s$^{-1}$), taken as 20°C. Three representative grain sizes were used; $D_{16}$, $D_{50}$, and $D_{84}$ of the active layer (Hoey & Ferguson, 1994) calculated by combining grain size distributions from five bulk surface and five bulk subsurface samples.

**Acknowledgements**

This research was undertaken as part of a United Kingdom Research and Innovation (UKRI) Natural Environment Research Council (NERC) and Department of Science and Technology - Philippine Council for Industry, Energy and Emerging Technology Research and Development (DOST-PCIEERD) – Newton Fund grant NE/S003312, and the Global Challenges Research Fund (GCRF) and Newton Fund Consolidation Account (GNCA) EP/X527749/1. We thank Craig McDonell, Esma Guardian, John Edward Perez, Catherine Sabillo and Juan Carlo Miguel Reyes. For the purpose of open access, the authors have applied a Creative Commons Attribution (CC BY) licence to any Author Accepted Manuscript version arising from this submission.

https://doi.org/10.5194/egusphere-2025-2722
Preprint. Discussion started: 7 July 2025


## Author contributions

Conceptualisation: LQ, TBH, RDW

Investigation: LQ, TBH, RDW

Methodology: LQ, TBH, RDW

Data curation: LQ, CM

Formal analysis: LQ

Visualisation: LQ

Writing – section draft and editing: LQ, TBH, RDW, RJB

Writing – manuscript review and editing: RDW, TBH, RJB, PMLT, CPCD

Funding acquisition: RDW, CPCD, TBH, PMLT

## Open research

Data used in this manuscript is available from https://gla-my.sharepoint.com/:f:/g/personal/richard_williams_glasgow_ac_uk/EkgMYz4UhH9Lsv8Rg60BftwBjS2ngnRtzIUidsGdDE4fXQ?e=wwp3fS Following peer review, these data will be made freely available from the UKRI-NERC Environment Information Data Centre (dataset currently under embargo during peer review).

## References

Adams, D.L. and Eaton, B.C.: A comparison of 1D and 2D bedload transport functions under high excess shear stress conditions in laterally constrained gravel-bed rivers: a laboratory study, Earth Surface Dynamics., 10, 895-907, https://doi.org/10.5194/esurf-10-895-2022, 2022.

Ancey, C.: Bedload transport: a walk between randomness and determinism. Part 2. Challenges and prospects, Journal of Hydraulic Research, 58, 18-33, https://doi.org/10.1080/00221686.2019.1702595, 2020.

Ancey, C. and Pascal, I.: Estimating mean bedload transport rates and their uncertainty, Journal of Geophysical Research: Earth Surface,125, e2020JF005534, https://doi.org/10.1029/2020JF005534, 2020.

Bates, P.D.: Flood Inundation Prediction, Annual Review of Fluid Mechanics, 54, 287-315, https://doi.org/https://doi.org/10.1146/annurev-fluid-030121-113138, 2022.

Boothroyd, R.J., Williams, R.D., Hoey, T.B., Brierley, G.J., Tolentino,P.L.M., Guardian, E.L., Reyes, J.C.M.O., Sabillo, C.J., Quick, L., Perez, J.E.G., and David, C.P.C.: Big data show idiosyncratic patterns and rates of geomorphic river mobility, Nature Communications, 16, 3263, https://doi.org/10.1038/s41467-025-58427-9, 2025.

Carbonneau, P. E., Fonstad, M. A., Marcus, W. A., and Dugdale, S. J.: Making riverscapes real, Geomorphology, 137, 74-86. https://doi.org/10.1016/j.geomorph.2010.09.030, 2012.

Church, M., and Jones, D.: Channel bars in gravel bed rivers, in Hey, R.D., Bathurst, J.C., and Thorne, C.R. (Eds): Gravel Bed Rivers: Fluvial Process, Engineering and Management, Wiley, Chichester, 291–339, 1982.

Dhont, B., and Ancey, C.: Are bedload transport pulses in gravel bed rivers created by bar migration or sediment waves? Geophysical Research Letters, 45, 5501–5508, https://doi.org/10.1029/2018GL077792, 2018.

Ettema, R., and Armstrong, D.L.: Bedload and channel morphology along a braided sand-bed channel: insights from a large flume. Journal of Hydraulic Research, 57, 822-35, doi: 10.1080/00221686.2018.1555557, 2019.

Galeazzi, C.P., Almeida, R.P., and do Prado, A.H.: Linking rivers to the rock record: Channel patterns and paleocurrent circular variance: Geology, 49, 1402-7. https://doi.org/10.1130/G49121.1,2021.

Ghilardi, T., Franca, M.J., and Schleiss, A.J.: Period and amplitude of bedload pulses in a macro-rough channel. Geomorphology, 221, 95-103. https://doi.org/10.1016/j.geomorph.2014.06.006, 2014.

Ghosh, K., Chakraborty, T., and Patel, P.P.: A new braiding index to assess river regulation effects in multi-thread channels: Insights from a highly regulated Himalayan River, River Research and Applications, 1-20, DOI: 10.1002/rra.4261, 2023.

Graf, W.L.: Locational probability for a dammed, urbanizing stream: Salt River, Arizona, USA, Environmental Management, 25, 321–335, DOI: 10.1007/s002679910025, 2000.

Hoey, T.B.: Temporal variations in sediment transport rates and sediment storage in gravel bed rivers, Progress in Physical Geography, 16, 319-38, 1992.

Hoey, T., Cudden, J., and Shvidchenko, A.: The consequences of unsteady sediment transport in braided rivers, In Mosley, M.P. (ed) Gravel-Bed Rivers V, New Zealand Hydrological Society, Wellington, New Zealand, 121-142, 2001.

Huang, H.Q.: Reformulation of the bed load equation of Meyer-Peter and Muller in light of the linearity theory for alluvial channel flow, Water Resources Research, 46, W09533, doi:10.1029/2009WR008974, 2010.

Huang, H.Q., and Nanson, G. C.: Why some alluvial rivers develop an anabranching pattern. Water Resources Research, 43, https://doi.org/10.1029/2006WR005223 , 2007.

https://doi.org/10.5194/egusphere-2025-2722
Preprint. Discussion started: 7 July 2025


Kasprak, A., Hough-Snee, N., Beechie, T., Bouwes, N., Brierley, G., Camp ,R., Fryirs, K., Imaki, H., Jensen, M., O'Brien, G., Rosgen, D., and Wheaton, J.: The Blurred Line between Form and Process: A Comparison of Stream Channel Classification Frameworks, PLoS ONE 11: e0150293, doi:10.1371/journal.pone.0150293, 2016.

Kastdalen, L., Stickler, M., Malmquist, C. and Heggenes, J.: Evaluating methods for measuring in-river bathymetry: Remote sensing green LIDAR provides high-resolution channel bed topography limited by water penetration capability, River Research and Applications, 40, 467-82. https://doi.org/10.1002/rra.4245, 2024.

Kostic, B., and Aigner, T.: Sedimentary architecture and 3D ground-penetrating radar analysis of gravelly meandering river deposits (Neckar Valley, SW Germany), Sedimentology, 54, 789-808, doi.org/10.1111/j.1365-3091.2007.00860.x, 2007.

Lague, D., and Feldmann, B.. Topo-bathymetric airborne LiDAR for fluvial-geomorphology analysis. In P. Tarolli and S.M. Mudd (Eds.): Developments in Earth Surface Processes, 23, 25-54, Elsevier, https://doi.org/https://doi.org/10.1016/B978-0-444-64177-9.00002-3, 2020.

Legleiter, C. J.: The optical river bathymetry toolkit. River Research and Applications, 37, 555-68, https://doi.org/10.1002/rra.3773, 2021.

Lisle, T.E., Nelson, J.M., Pitlick, J. Madej, M.A., and Barkett, B.L.: Variability of bed mobility in natural, gravel-bed channels and adjustments to sediment load at local and reach scales, Water Resources Research, 36, 3743-55, 2000.

Lisle, T.E., Pizzuto, J.E., Ikeda, H., Iseya, F., and Kodama, Y.: Evolution of a sediment wave in an experimental channel, Water Resources Research, 33, 1971-81, 1997.

Marchetti, G., Bizzi, S., Belletti, B., Lastoria, B., Comiti, F., and Carbonneau, P.E.: Mapping riverbed sediment size from Sentinel-2 satellite data, Earth Surface Processes and Landforms, DOI: 10.1002/esp.5394, 2022

Nicholas, A.P.: Modelling bedload yield in braided gravel bed rivers, Geomorphology, 36, 89-106, 2000.

Paola, C.: Incoherent structure: turbulence as a metaphor for stream braiding, In Ashworth, P.J. Bennett, S.J. Best, J.L., and McLelland, S.J. (eds): Coherent Flow Structures in Open Channels, Chichester, Wiley, 705-723, 1996

Piégay, H., Arnaud, F., Belletti, B., Bertrand, M., Bizzi, S., Carbonneau, P., Dufour, S., Liébault, F., Ruiz-Villanueva, V., and Slater, L.: Remotely sensed rivers in the Anthropocene: state of the art and prospects, Earth Surface Processes and Landforms, 45, 157-188, https://doi.org/https://doi.org/10.1002/esp.4787, 2020.

Quick, L., Williams, R.D., Boothroyd, R.J., Hoey, T.B., Tolentino, P.L.M., MacDonell, C.J., Guardian, E.L., Reyes, M., Sabilio, C.J.L., Perez, J.E.G., and David, C.P.C.: Confined and mined: anthropogenic river modification as a driver of flood risk change, npj Natural Hazards, 2, https://doi.org/10.1038/s44304-024-00051-6, 2025.

Recking, A.: An analysis of nonlinearity effects on bed load transport prediction, Journal of Geophysical Research, 118, 20090, https://doi.org/10.1002/jgrf.20090, 2013.

https://doi.org/10.5194/egusphere-2025-2722
Preprint. Discussion started: 7 July 2025


Recking, A., Liébault, F., Peteuil, C., and Jolimet, T.: Testing bedload transport equations with consideration of time scales, Earth Surface Processes and Landforms, 37, 774–789, doi: 10.1002/esp.3213, 2012.

Redolfi, M., Bertoldi, W., Tubino, M., and Welber, M.: Bed load variability and morphology of gravel bed rivers subject to unsteady flow: A laboratory investigation. Water Resources Research, 54, 842–862, https://doi.org/10.1002/2017WR021143, 2018.

Reid, H.E., Williams, R.D., Brierley, G.J., Coleman, S.E., Lamb, R., Rennie, C.D., and Tancock, M.J.: Geomorphological effectiveness of floods to rework gravel bars: Insight from hyperscale topography and hydraulic modelling. Earth Surface Processes and Landforms, 44, 595–613, https://doi.org/10.1002/esp.4521, 2019.

Reiterer, K., Gold, T., Hauer, C., Habersack, H., and Sindelar, C.: On the longitudinal and transverse advection and dispersion of bed load pulses induced by a local sediment surplus. Journal of Geophysical Research: Earth Surface,130, e2024JF007986, https://doi.org/10.1029/2024JF007986, 2025.

Rice, S.P., and Church, M.: Grain-size sorting within river bars in relation to downstream fining along a wandering channel. Sedimentology, 57, 232-51, https://doi.org/10.1111/j.1365-3091.2009.01108.x(2009).

Schwendel, A.C., Death, R.G., and Fuller, I.C.: The assessment of shear stress and bed stability in stream ecology, Freshwater Biology 55, 261-81, doi:10.1111/j.1365-2427.2009.02293.x, 2010.

Segura, C., and Pitlick, J.: Coupling fluvial-hydraulic models to predict gravel transport in spatially variable flows, Journal of Geophysical Research: Earth Surface, 120, 834-855, https://doi.org/https://doi.org/10.1002/2014JF003302, 2015.

Tejedor, A., Schwenk, J., Kleinhans, M., Limaye, A. B., Vulis, L., Carling, P., Kantz, H., and Foufoula-Georgiou, E.: The entropic Braiding Index (eBI): A robust metric to account for the diversity of channel scales in multi-thread rivers, Geophysical Research Letters, 49, e2022GL099681. https://doi.org/10.1029/2022GL099681, 2022.

Tolentino, P.L.M., Williams, R., and Hurst, M.: Hydraulic and geomorphic assessment of structural interventions on the tropical, wandering Bislak River, the Philippines. River Research and Applications, 1-18, https://doi.org/10.1002/rra.4362, 2024.

Wilcock. P., Pitlick. J., and Cui. Y.: Sediment transport primer: estimating bed-material transport in gravel-bed rivers, General Technical Report RMRS-GTR-226, Fort Collins, CO: U.S. Department of Agriculture, Forest Service, Rocky Mountain Research Station, 78, 2009.

Williams, R. D., Rennie, C.D., Brasington, J., Hicks, D.M., and Vericat, D.: Linking the spatial distribution of bed load transport to morphological change during high-flow events in a shallow braided river, Journal of Geophysical Research Earth Surface, 120, 604–622. doi:10.1002/2014JF003346, 2015.